T. Grisa, *et al.*: On a Multidimensional Data Proessing Method for Radiation ...
Nuclear Technology & Radiation Protection: Year 2020, Vol. 35, No. 3, pp. 235-243

235

ON A MULTIDIMENSIONAL DATA PROCESSING METHOD FOR RADIATION PORTAL MONITORS

by

Tomas GRISA[1*], *Daniel SAS*[2], *and Lubomir GRYC*[3]

[1] NUVIA a.s., Trebic, Czech Republic
[2] NBC Defence Institute, University of Defence, Vyskov, Czech Republic
[3] National Radiation Protection Institute, Prague, Czech Republic

From a homeland security point of view, it is important to detect the transportation of radioactive materials or potential radioactive contamination. The most commonly used devices are radiation portal monitors with plastic scintillation detectors. A signal from such detectors is processed by an amplitude analyser which can separate pulses into several mutually independent energy windows (representing energy intervals of gamma radiation). Therefore, the most appropriate method of evaluation is by the use of algorithms for multidimensional processing. This article describes a novel generalised approach designed with respect to the properties of radiation portal monitors. It includes a description of formulas and a whole algorithm as well as the procedure for determining the appropriate critical and detection limits. The predicted probability distribution for the proposed method of calculation was verified by simulations and experimental measurements. The algorithm was also compared with a commonly used gross counting algorithm.

Key words: radiation portal monitor, multidimensional data processing, critical limit, detection limit, scintillation detector, amplitude analyser

INTRODUCTION

Even though there are many different algorithms for lowering detection limits [1-3] and a basic identification of measured nuclides [4, 5] in the field of radiation portal monitors, the most commonly used approach is the direct gross counting of pulses in each energy window (or their sum) independently. The idea of this algorithm is based on a fact, that the radioactive decay follows a Poisson distribution [6]. More-over, for high count rates the Poisson distribution can be approximated by a normal distribution [7, 8]

$$Po(\lambda) \quad N(\lambda,\lambda), \quad \text{for } \lambda \quad \infty \qquad (1)$$

This is the consequence of the central limit theorem allowing the measured data to be processed as a test of the parameters of a normal distribution. To begin with, it is important to estimate the parameters of the random variability of background radiation B $N(\mu_B, \mu_B)$. Because the sample mean is an unbiased estimator of the population mean, the value μ_B can be estimated as a sample mean from a sufficient number of measured values of background radiation.

The normal random variable, B, then describes the stochastic behaviour of background radiation. With respect to the properties of the normal distribution, a *critical limit* (decision threshold) L_C is calculated according to [9] and ISO 11929:2010 [10] as

$$L_C \quad \mu_B \quad k_{1\ \alpha} \sqrt{\mu_B} \qquad (2)$$

where $k_{1\ \alpha}$ is the quantile of the standard normal distribution for probability $1 - \alpha$. The value α specifies the probability of false alarms being caused by natural variations in the background radioactivity.

An object is then said to be radioactive if the measured number of pulses is greater than L_C [9]. Furthermore, it is important to calculate the *detection limit* L_D [9, 10], which describes the minimum number of pulses required for an object to be said to be radioactive with a pre-set probability $(1 - \beta)$. The relationship between L_C and L_D is illustrated in fig. 1. With respect to eq. (1), the following equation holds true

$$L_D \quad L_C \quad k_{1\ \beta} \sqrt{L_D} \qquad (3)$$

The value L_D is then for a simple gross counting algorithm (GCA) calculated as the positive root of the following quadratic equation

* Corresponding author; e-mail: tomas.grisa@nuvia.com

236

T. Grisa, *et al.*: On a Multidimensional Data Proessing Method for Radiation ...
Nuclear Technology & Radiation Protection: Year 2020, Vol. 35, No. 3, pp. 235-243
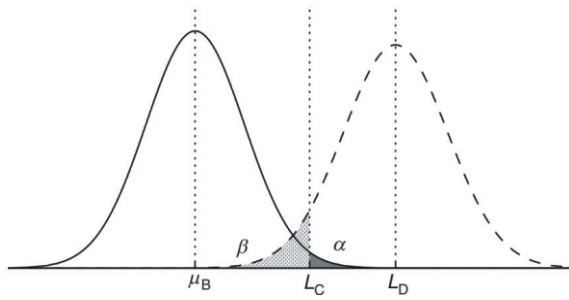
Figure 1. The relationship between a critical limit L_C and a detection limit L_D

$$L_D^2 \quad L_D\,(2L_C \quad k_{1-\beta}^2) \quad L_C^2 \quad 0 \tag{4}$$

ALGORITHM DESIGN

When processing a signal from a plastic scintillation detector using an amplitude analyser with more mutually independent energy windows, it is important to use algorithms for multidimensional data processing. If the energy windows are evaluated independently with a GCA, then it is not straightforward to set a false alarm rate as well as to define the detection limits of a whole system.

Let us assume an amplitude analyser with n mutually independent energy windows, where the number of counts in each channel is represented by a normal random variable X_1, ..., X_n. Together, they are represented by an n-dimensional normal random variable (random vector) $\mathbf{X}$ with the following probability density function Σ

$$f_\mathbf{x}(\mathbf{x}) \quad \frac{1}{\sqrt{(2\pi)^n |\Sigma|}} \exp \quad \frac{1}{2}(\mathbf{x}\ \mu)^T \Sigma^{-1}(\mathbf{x}\ \mu) \tag{5}$$

where

$$\mu \quad \begin{matrix} \mu_{X_1} \\ \vdots \\ \mu_{X_n} \end{matrix} \tag{6}$$

is a mean vector and the following matrix Σ is a covariance matrix with variances equal to $\mu_{X_1}, \ldots, \mu_{X_n}$ on its diagonal and the off-diagonal elements are equal to zero.

$$\Sigma \quad \begin{matrix} \mu_{X_1} & 0 & \ldots & 0 \\ 0 & \mu_{X_2} & \ldots & 0 \\ \vdots & \vdots & \ddots & \vdots \\ 0 & 0 & \ldots & \mu_{X_n} \end{matrix} \tag{7}$$

The zero values of the off-diagonal correlation coefficients are a consequence of independent random variables X_1, ..., X_n. This assumption is natural, because even if a nuclide with multiple energy lines per

disintegration is measured, the resulting gamma photons are independent – if one such gamma photon is detected, it does not guarantee that others must be detected as well. However, if they were to be detected together (from the same disintegration) they would be summed together. Although the count rate would be increased in multiple windows, they are statistically independent. Moreover, the assumption of zero correlations is the same as for the gamma spectrum, where all channels are not correlated – otherwise the total count rate of the spectra would not follow the Poisson distribution.

Now, let us calculate the distance of each measured point $\mathbf{x}$ from a n-dimensionl space to point $\mu\ [\mu_{X_1}, \ldots, \mu_{X_n}]$ by using the Mahalanobis distance [11]

$$D(\mathbf{x}, \mu) \quad \sqrt{\sum_{i=1}^{n} \frac{(x_i\ \mu_{X_i})^2}{\mu_{X_i}}} \tag{8}$$

The random variable calculated as $D(\mathbf{x}, \mu)^2$ follows an χ^2 distribution with n degrees of freedom. Therefore a n-dimensional confidence region which would include $(1-\alpha)\,100\,\%$ of the measured values is represented by an n-dimensional ellipsoid. However, the confidence region would exclude those cases in which the measured values are much smaller than their mean values. But this is undesirable – we are interested in cases where measured pulses are higher than background radiation. Therefore, let us assume the following modification of the distance calculation, which creates the random variable Y

$$Y \quad D^*(\mathbf{x}, \mu) \quad \sqrt{\sum_{i=1}^{n} \frac{(\max(x_i\ \mu_{X_i}, 0))^2}{\mu_{X_i}}} \tag{9}$$

The calculation of a cumulative distribution function of such a random variable is not straightforward due to the $\max(x_i\ \mu_{X_i}, 0)$ term in eq. (9). The sample space has to be divided into 2^n disjoint regions and the resulting cumulative distribution function is obtained as a sum of a cumulative distribution function for each region.

To illustrate how the cumulative distribution function is derived, let us assume $n = 2$ and the following equation, where the right-hand side represents the probability that the random variable Y takes on a value less than or equal to y

$$F_Y(y) \quad P(Y\ y) \quad 1 \quad P(Y\ y) \tag{10}$$

As described, the sample space has to be divided into the following disjoint regions.

Region $x_1 \quad \mu_{X_1}, x_2 \quad \mu_{X_2}$

The eq. (11) describes the probability for the union of events that $Y > y$ together with $X_1 \quad \mu_{X_1}$ and $X_2 \quad \mu_{X_2}$, which can be rewritten in the form of a conditional probability.

T. Grisa, *et al.*: On a Multidimensional Data Proessing Method for Radiation ...
Nuclear Technology & Radiation Protection: Year 2020, Vol. 35, No. 3, pp. 235-243

237

$$P(Y \ y) \ P(Y \ y \cap X_1 \ \mu_{X_1} \cap X_2 \ \mu_{X_2})$$
$$P(X_1 \ \mu_{X_1}) \ P(X_2 \ \mu_{X_2})$$
$$P(Y \ y \mid X_1 \ \mu_{X_1} \cap X_2 \ \mu_{X_2})$$
$$\frac{1}{2} \frac{1}{2} P(0 \ y \mid X_1 \ \mu_{X_1} \cap X_2 \ \mu_{X_2})$$
$$\frac{1}{2} \frac{1}{2} P(0 \ y) \tag{11}$$

Because the resulting distance is in this region always equal to zero, then the conditional probability is equal directly to $P(0 > y)$. The result is for this region described by the eq. (12)

$$P(Y \ y) \quad \begin{cases} 1/4, & \text{for } y \ 0 \\ 0, & \text{for } y \ 0 \end{cases} \tag{12}$$

Region $x_1 \ \mu_{X_1}, x_2 \ \mu_{X_2}$

For this region the modified distance calculation is affected only by x_1, therefore the resulting random variable Y over this region follows the standard normal distribution. However, the conditional probability for modified distance over this region is not equal directly to $1 - (y)$, where is a cumulative distribution function of the standard normal distribution, but must be rescaled by the correction factor 2, because $(1 - (y))$ gives in this region values from 0 only to 1/2

$$P(Y \ y) \ P(Y \ y \cap X_1 \ \mu_{X_1} \cap X_2 \ \mu_{X_2})$$
$$P(X_1 \ \mu_{X_1}) \ P(X_2 \ \mu_{X_2})$$
$$P(Y \ y \mid X_1 \ \mu_{X_1} \cap X_2 \ \mu_{X_2}) \ \frac{1}{2} \frac{1}{2}$$
$$P((X_1 \ \mu_{X_1})/\sqrt{\mu_{X_1}} \ y \mid X_1 \ \mu_{X_1} \cap X_2 \ \mu_{X_2}) \tag{13}$$

$$P(Y \ y) \quad \begin{cases} \dfrac{1}{4}, & \text{for } y \ 0 \\ \dfrac{1}{2}(1 \ \Phi(y)), & \text{for } y \ 0 \end{cases} \tag{14}$$

Region $x_1 \ \mu_{X_1}, x_2 \ \mu_{X_2}$

This region is similar as in the previous case.

$$P(Y \ y) \ P(Y \ y \cap X_1 \ \mu_{X_1} \cap X_2 \ \mu_{X_2})$$
$$P(X_1 \ \mu_{X_1}) \ P(X_2 \ \mu_{X_2})$$
$$P(Y \ y \ X_1 \ \mu_{X_1} \cap X_2 \ \mu_{X_2}) \ \frac{1}{2} \frac{1}{2}$$
$$P((X_2 \ \mu_{X_2})/\sqrt{\mu_{X_2}} \ y \ X_1 \ \mu_{X_1} \cap X_2 \ \mu_{X_2}) \tag{15}$$

$$P(Y \ y) \quad \begin{cases} \dfrac{1}{4}, & \text{for } y \ 0 \\ \dfrac{1}{2}[1 \ \Phi(y)], & \text{for } y \ 0 \end{cases} \tag{16}$$

Region $x_1 \ \mu_{X_1}, x_2 \ \mu_{X_2}$

Only in this region is the modified distance calculation affected by both x_1 and x_2. Therefore, the resulting random variable Y over this region follows χ^2 distribution with two degrees of freedom. The result for this region described by the eq. (18), where G is a cumulative distribution function of χ^2 distribution with two degrees of freedom.

$$P(Y \ y) \ P(Y \ y \cap X_1 \ \mu_{X_1} \cap X_2 \ \mu_{X_2})$$
$$P(X_1 \ \mu_{X_1}) \ P(X_2 \ \mu_{X_2})$$
$$P(Y \ y \mid X_1 \ \mu_{X_1} \cap X_2 \ \mu_{X_2}) \ \frac{1}{2} \frac{1}{2}$$
$$P(\sum_{i \ 1}^{2}(X_i \ \mu_{X_i})^2/\sqrt{\mu_{X_i}} \ y^2 \mid X_1 \ \mu_{X_1} \cap X_2 \ \mu_{X_2}) \tag{17}$$

$$P(Y \ y) \quad \begin{cases} \dfrac{1}{4}, & \text{for } y \ 0 \\ \dfrac{1}{4}(1 \ G(y^2,2)), & \text{for } y \ 0 \end{cases} \tag{18}$$

The resulting cumulative distribution function for case $n = 2$ is given as

$$P(Y \ y) \quad \begin{cases} 1, & \text{for } y \ 0 \\ (1 \ \Phi(y)) \ \dfrac{1}{4}(1 \ G(y^2, 2)), & \text{for } y \ 0 \end{cases} \tag{19}$$

$$F_Y(y) \ P(Y \ y)$$
$$\begin{cases} 0, & \text{for } y \ 0 \\ 1 \ [1 \ \Phi(y) \ \dfrac{1}{4}(1 \ G(y^2, 2))], & \text{for } y \ 0 \end{cases} \tag{20}$$

For the general dimension n, there will always be n regions, where the resulting random variable Y follows the standard normal distribution. The area of each region is equal to $1/2^n$ and because the correction factor 2 must be applied, then $n/2^{n-1} ([1 - (y))$ represents these regions. For other regions, the resulting random variable Y follows the χ^2 distribution with various degrees of freedom. The number of such regions (for i representing the degrees of freedom) is equal to $\binom{n}{i}$. Therefore,

$$\frac{\sum_{i \ 2}^{n}\binom{n}{i}}{2^n}(1 \ G(y^2,i))$$

represents all such regions. The last region is equal to zero, because it represents the cases, when values in all random variables are less than their mean values. Therefore, in general, the cumulative distribution function of the proposed random variable Y is consequently given as the following eq.
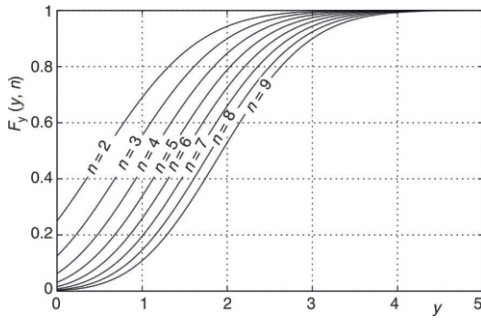
Figure 2. Cumulative distribution functions for $n = 2, ..., 9$

$$F_Y(y, n)$$

$$0, \qquad \text{for } y \le 0$$

$$1 - \frac{n}{2^{n-1}}(1 - \Phi(y)) - \sum_{i=2}^{n} \frac{\binom{n}{i}}{2^n}(1 - G(y^2, i))$$

$$\text{for } y > 0 \qquad (21)$$

Figure 2 illustrates the derived cumulative distribution function for $n = 2, ..., 9$. A measured object is therefore said to be radioactive if the following equation holds true

$$D^*(\mathbf{x}, \mu) \ge k^*_{1-\alpha}(n) \qquad (22)$$

where $k^*_{1-\alpha}(n)$ is a quantile of the derived distribution. Commonly used quantiles were numerically calculated and are stated in tab. 1.

According to the ISO 11929:2010 [10], a set of x, for which $D^*(\mathbf{x}, \mu) = k^*_{1-\alpha}(n)$ holds true defines a n-dimensional analogy of L_C. This is illustrated for $n = 2$ in fig. 3 for various values of α.

If we are also looking for a n-dimensional analogy of L_D, then it is defined as a set of n-tuples $[\delta_1, ..., \delta_n]$, forming n-dimensional manifolds (in 2 dimensions: curves), parameterized by α and β, for which the following equation holds true

$$\underset{\Omega}{\int \cdots \int} \frac{1}{\sqrt{(2\pi)^n |\Sigma_\delta|}}$$

$$\exp\left[-\frac{1}{2}(\mathbf{x} - \mu_\delta)^T \Sigma_\delta^{-1}(\mathbf{x} - \mu_\delta)\right] d\mathbf{x} = \beta \qquad (23)$$
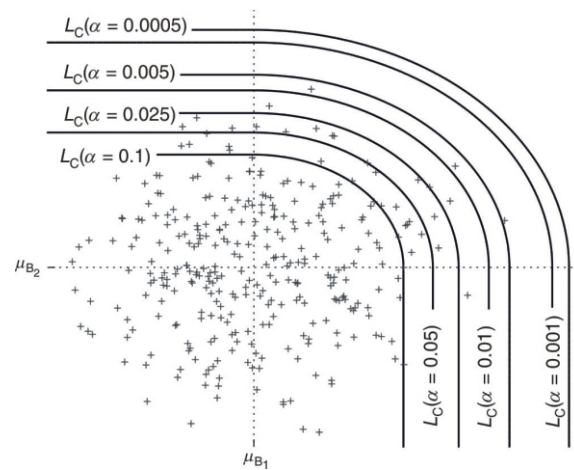
Figure 3. Relationship between L_C and L_D. Analogy of L_C for $n = 2$

where

$$\mu_\delta = \begin{pmatrix} \delta_1 \\ \vdots \\ \delta_n \end{pmatrix} \qquad (24)$$

$$\Sigma_\delta = \begin{pmatrix} \delta_1 & 0 & \cdots & 0 \\ 0 & \delta_2 & \cdots & 0 \\ \vdots & \vdots & \ddots & \vdots \\ 0 & 0 & \cdots & \delta_n \end{pmatrix} \qquad (25)$$

and Ω is a set, for which $D^*(\mathbf{x}, \mu) < k^*_{1-\alpha}(n)$ holds true. In general, an analytic calculation of such n-tuples is difficult. Therefore, eq. (23) has to be solved numerically. Another numerical approoch ispresented in the Annex. The 2-D analogies of L_D for $\alpha = 0.01$ and various values β are illustrated in fig. 4.

Figure 5 illustrates a global case with 2-D analogies of L_C and L_D. It illustrates values of background radiation (the random variable B) as well as values of a measured object (the random variable X), which lies directly on the threshold L_D. The values of background radiation will lie beyond the borderline L_C with the pre-set probability α (false alarms). In contrast, the values of a measured object will lie in front of the borderline L_C with the preset probability β, which means that L_D is the threshold line indicating the lowest value which can be detected with $1 - \beta$ probability.

Table 1. Table of quantiles $k^*_{1-\alpha}(n)$ for $n = 2, ..., 9$

n	$1 - \alpha$						
	0.90	0.95	0.975	0.99	0.995	0.999	0.9995
2	1.7183	2.0568	2.3531	2.6999	2.9374	3.4297	3.6222
3	2.0025	2.3312	2.6194	2.9574	3.1892	3.6707	3.8593
4	2.2260	2.5491	2.8325	3.1652	3.3935	3.8681	4.0541
5	2.4156	2.7349	3.0151	3.3441	3.5699	4.0394	4.2235
6	2.5829	2.8995	3.1772	3.5034	3.7274	4.1930	4.3757
7	2.7342	3.0487	3.3246	3.6486	3.8710	4.3336	4.5150
8	2.8735	3.1863	3.4606	3.7828	4.0039	4.4639	4.6443
9	3.0030	3.3144	3.5875	3.9082	4.1282	4.5860	4.7656

T. Grisa, *et al*.: On a Multidimensional Data Proessing Method for Radiation ...
Nuclear Technology & Radiation Protection: Year 2020, Vol. 35, No. 3, pp. 235-243

239
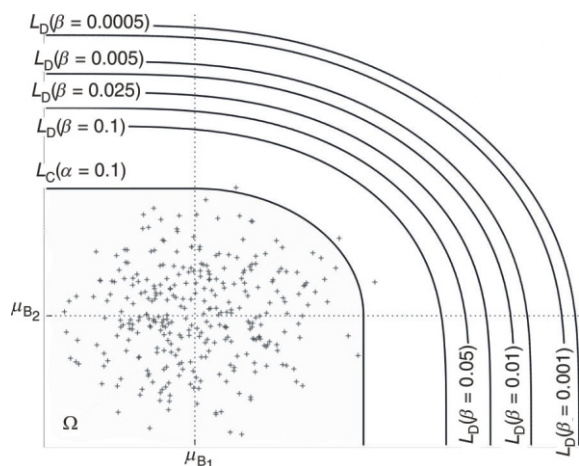
Figure 4. Relationship between L_C and L_D. Analogy of L_D for $n = 2$
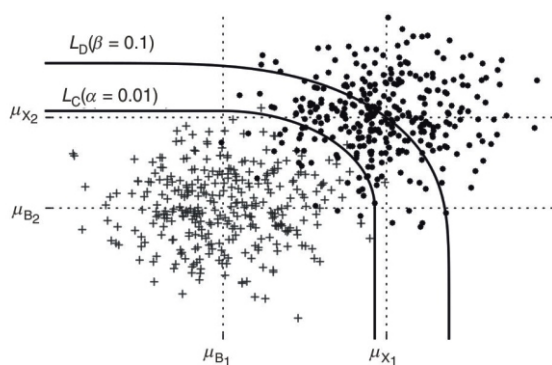
Figure 5. Relationship between L_C and L_D for $n = 2$

Figure 6. Comparison of the proposed algorithm (bold line) and the evaluation of each channel independently (dashed line). The diagonal line represents the auxiliary summary channel. Probability $\alpha = 0.01$
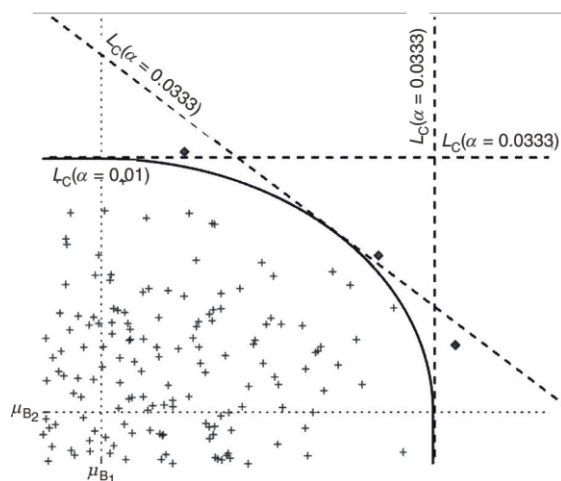
Figure 7. Comparison of the proposed algorithm (bold line) and the evaluation of each channel independently (dashed line). The diagonal line represents the auxiliary summary channel. Probability $\alpha = 0.00333$

The advantage of the suggested approach of data evaluation from an amplitude analyzer with more energy windows is the direct control over the values α and β which leads to precise calculation of critical and detection limits. The difference between the suggested approach and the evaluation of data from each channel independently by a GCA can be seen in fig. 6 and fig. 7, where the bold line represents L_C for the suggested approach and the dashed lines represent the evaluation of each channel independently. For illustrative purposes $n = 2$.

The first case shows the situation in which the value of L_C is calculated for each channel independently with the probability $\alpha = 0.01$. The diagonal line (which is inclined according to the relative contribution of both channels to the total count rate) represents L_C for an auxiliary summary channel (often used for an additional reduction of detection limits, because it represents a total count of impulses from a detector). In this case (fig. 6) the lower detection limits are reached but at the cost of a higher ratio of false alarms – three channels, each with the probability $\alpha = 0.01$. Therefore, the total ratio of false alarms is 3 cases out of each 100 measurements (in this particular example 9 cases of total 300 measurements – highlighted by a rhombus mark).

The second case shows a similar situation, however the probability $\alpha = 0.01/3 = 0.00333$ is used for each channel, where the divisor 3 represents the total number of channels (together with an auxiliary summary channel), which are evaluated independently (using this assumption helps to achieve the same amount of false alarms as for the proposed approach with $\alpha = 0.01$). Figure 7 shows the direct comparison of a calculated threshold L_C for the suggested approach and the simple evaluation of each channel independently.

PROBABILITY DISTRIBUTION VALIDATION

A random number simulation was used to test the suggested approach. Four sets of random values (each

240

T. Grisa, *et al.*: On a Multidimensional Data Proessing Method for Radiation ...
Nuclear Technology & Radiation Protection: Year 2020, Vol. 35, No. 3, pp. 235-243

of 5000 observations) with the normal distribution $X_1 = N(\mu_1, \mu_1), ..., X_4 = N(\mu_4, \mu_4)$ with known parameters $\mu_1,..., \mu_4$ were generated for the purposes of a simulation. Then $D^*(\mathbf{x}, \mu)$ was calculated according to eq. (9) for each quadruple. The Kolmogorov-Smirnov test [12] with the null hypothesis that the sample comes from the hypothesised distribution was used to test if the calculated values have the predicted distribution defined by (21). Based on the result p-value = 0.677, the null hypothesis is not rejected at a significance level $\alpha = 0.05$.

In addition, real experimental data were acquired with NuSAFEGATE, which is used as a hidden radiation portal monitor for pedestrian monitoring and was developed by NUVIATech Instruments. This detection module contains a 4-channel digital counter and a 1.6 l (100 × 4 × 4 cm) polystyrene-based plastic scintillation detector. The detection energy range is up to 2 MeV of gamma radiation. Because the Compton scattering is the dominant mechanism for photon energy deposition in plastic scintillators ([13-15]), boundaries of all energy windows were set according to [4]. The energy ranges of absorbed gamma radiation for all four energy windows (EW1 to EW4) are listed in tab. 2.

For this experiment, counts in each energy window were recorded with a period of 250 ms. The values $\mu_{X_2}, ... \mu_{X_4}$ were calculated as a sample mean from 7200 samples (30 minutes). Then another 5000 samples were acquired and for each sample the value $D^*(\mathbf{x}, \mu)$ was calculated according to eq. (9). Finally, the Kolmogorov-Smirnov test was performed as for the random number simulation. Based on the result p-value = 0.341, the null hypothesis is not rejected at a significance level $\alpha = 0.05$. Results of both tests are graphically illustrated by Q-Q plots in figs. 8 and 9.

COMPARISON WITH THE COMMONLY USED METHOD

The performance of the proposed algorithm was experimentally compared to the commonly used GCA. This experiment was conducted with sources listed in tab. 3. The sources were placed one at a time at a 0.5 m distance from the front cover of the detection module and 100 samples were acquired for each source. The acquisition period was set to 1 second. The gross background counts are listed in tab. 4 and the net counts per second per kBq at a 0.5 m distance for each energy window are presented in tab. 5.

Based on the measured values, the critical and decision limits were calculated for each radionuclide according to the eqs. (22) and (23) with probabilities

Table 2. The energy ranges of absorbed gamma radiation for each energy window

EW1 [MeV]	EW2 [MeV]	EW3 [MeV]	EW4 [MeV]
0.04-0.24	0.24-0.63	0.63-1.45	1.45-2.0
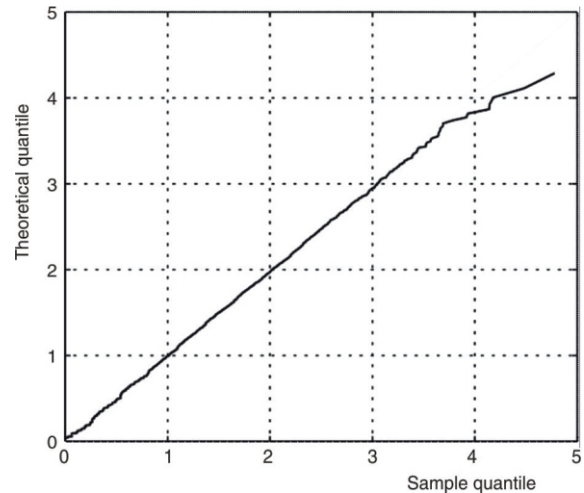
Figure 8. The Q-Q plot of a random number of a simulated and predicted distribution
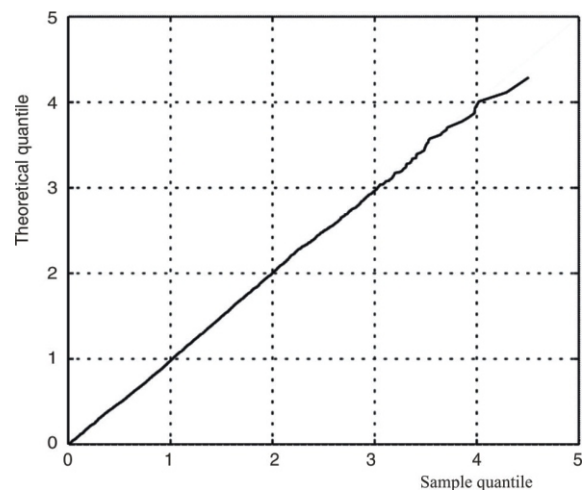
Figure 9. The Q-Q plot of measured and predicted distribution

Table 3. List of used sources with activities

Nuclide	Reference date	Reference activity [kBq]	Activity [kBq]
^{137}Cs	01.07.2015	881.1	789.857
^{60}Co	01.07.2015	849.9	455.558
^{241}Am	01.07.2015	864.5	857.950
^{134}Cs	31.12.2018	524.5	346.102
^{152}Eu	31.12.2018	447.9	420.381
^{133}Ba	31.12.2018	83.76	77.191

Table 4. Gross background counts per second (cps) for each energy window

EW1 [cps]	EW2 [cps]	EW3 [cps]	EW4 [cps]
512.50	134.22	73.81	18.55

$\alpha = 0.01$ and $\beta = 0.1$. In addition, the critical and decision limits were calculated for the GCA according to the eqs. (2) and (3) with $\alpha = 0.01/5 = 0.002$ and $\beta = 0.1$ for all four measured energy windows and one win-

T. Grisa, *et al.*: On a Multidimensional Data Proessing Method for Radiation ...
Nuclear Technology & Radiation Protection: Year 2020, Vol. 35, No. 3, pp. 235-243

241

Table 5. Net counts per second (cps) per kBq at a 0.5 m distance for each energy window

Nuclide	EW1 [cps]	EW2 [cps]	EW3 [cps]	EW4 [cps]
^{137}Cs	1.042	0.715	0.224	0.022
^{60}Co	1.329	1.152	1.115	0.262
^{134}Cs	2.577	1.812	0.631	0.080
^{152}Eu	2.045	0.800	0.439	0.090
^{133}Ba	2.461	0.446	0.045	0.008
^{241}Am	0.208	0.006	0	0

Table 6. Detection limits as MDA in kBq for the proposed algorithm (D^*) and a simple GCA with a non-detection probability $\beta = 0.1$ for overall evaluation with all energy windows together and for each energy window separately

	^{137}Cs	^{60}Co	^{134}Cs	^{152}Eu	^{133}Ba	^{241}Am
D^*	51.3	22.5	20.1	32.5	36.8	470.3
GCA overall	53.4	25.3	21.0	33.4	36.5	455.5
GCA separately	57.8	30.0	22.7	34.3	39.1	464.9

Table 7. Decrease or increase of MDA as a percentage when the proposed algorithm is used instead of a simple GCA

^{137}Cs	^{60}Co	^{134}Cs	^{152}Eu	^{133}Ba	^{241}Am
−3.93 %	−11.07 %	−4.29 %	−2.69 %	−0.82 %	−3.25 %

dow representing total counts. However, this approach does not give the overall performance of the whole system with more energy windows, because the auxiliary summary channel is correlated with other channels. Therefore, the detection limits with an overall non- detection probability $\beta = 0.1$ for all four measured energy windows and one window representing total counts were numerically established as well.

The detection limits as the minimum detectable activities (MDA) in kBq according to the ISO 11929:2010 [10] are presented in tab. 6 for the proposed algorithm and a GCA. It can be seen that the true MDA for an overall GCA is generally lower than direct calculation of MDA for each energy window separately. Moreover, the direct comparison between the proposed algorithm and a GCA is presented in tab. 7. The values describe the decrease or increase of MDA as a percentage when the proposed algorithm is used instead of a simple GCA.

It can be seen that the proposed algorithm brings improvement of detection limits for radionuclides with higher energies, which significantly contributes to more than two energy windows. Therefore, the most significant decrease of MDA was achieved for ^{60}Co. On the other hand, an increase of the MDA was observed only for ^{133}Ba and ^{241}Am, because their contribution is significant only in the first two energy windows, which can be seen in tab. 5.

CONCLUSION

The new generalised algorithm presented in this work, based on a multidimensional data analysis, is shown to work properly for the purposes of data evaluation from radiation portal monitors. Tests were presented for simulated and measured data, showing that the algorithm provides accurate critical and detection limits, which correspond to the statistical behaviour of measured data from radiation portal monitors. Moreover, the comparison with the commonly used GCA revealed that it can decrease detection limits for radionuclides, which significantly contributes to more than two energy windows. The proposed algorithm not only brings the simple combination of various energy windows into one resulting outcome (this reduces the amount of data, which are typically transmitted to an operating centre and are stored for further investigation), but also the immediate control over the ratio of false alarms and a proper method for calculating the critical and detection limits of the whole system. Therefore, it is appropriate for simple hidden radiation portal monitors, which were developed by NUVIATech Instruments. On the other hand, the approach to calculate the MDA for various nuclides is not straightforward and easy. However, normally there is no need to calculate them during each measurement. The MDA for portal monitors are typically calculated only as a system characterization for new geometries and various ambient radiation backgrounds.

ACKNOWLEDGMENT

AUTHORS' CONTRIBUTIONS

The idea for the study was put forward by T. Grísa, who also derived all the theoretical calculations, prepared the data evaluation, result interpretation and wrote the paper. The measurements were carried out by L. Gryc and D. Sas, who also made valuable contributions in various phases of this work.

REFERENCES

[1] Presti, C. A. L., *et al.*, Baseline Suppression of Vehicle Portal Monitor Gamma Count Profiles: A Characterization Study, Nuclear Instruments and Methods in Physics Research Section A: Accelerators, Spectrometers, *Detectors and Associated Equipment, 562* (2006), 1, pp. 281-297

[2] Ely, J., *et al.*, The Use of Energy Information in Plastic Scintillator Material, *Journal of Radioanalytical and Nuclear Chemistry, 276* (2008), 3, pp. 743-748

242

T. Grisa, *et al.*: On a Multidimensional Data Proessing Method for Radiation ...
Nuclear Technology & Radiation Protection: Year 2020, Vol. 35, No. 3, pp. 235-243

[3] Grisa, T., *et al.*, On the Ratio Distribution of Energy Windowing Algorithms for Radiation Portal Monitors, *Applied Radiation and Isotopes, 132* (2018), Feb.,, pp. 195-199

[4] Hevener, R., *et al.*, Investigation of Energy Windowing Algorithms for Effective Cargo Screening with Radiation Portal Monitors, *Radiation Measurements, 58* (2013), Nov., pp. 113-120

[5] Ely, J., *et al.*, The Use of Energy Windowing to Discriminate SNM from NORM in Radiation Portal Monitors, Nuclear Instruments and Methods in Physics Research Section A: Accelerators, Spectrometers, *Detectors and Associated Equipment, 560* (2006), 2, pp. 373-387

[6] L'Annunziata, M., *Handbook of Radioactivity Analysis*, 3rd ed., Elsevier, Oxford, UK, 2012

[7] Feller, W., *An Introduction to Probability Theory and Its Applications*, 3rd ed., John Wiley, New York, USA, 1968

[8] Wackerly, D., *et al.*, *Mathematical Statistics with Applications*, 7th ed., Thomson Brooks/Cole, Belmont, Tenn, USA, 2008

[9] Gilmore, G., *Practical Gamma-Ray Spectrometry*, 2nd ed., Wiley, Hoboken, N. J., USA, 2008

[10] ***, International Organization for Standardization (ISO), Determination of the Characteristic Limits (Decision Threshold, Detection Limit and Limits of the Confidence Interval) for Measurements of Ionizing Radiation – Fundamentals and Application, ISO 11929, ISO, Geneva, 2010

[11] Everitt, B., *et al.*, *Applied Multivariate Data Analysis*, 2nd ed., Oxford University Press, New York, USA, 2001

[12] James, F., *Statistical Methods in Experimental Physics*, 2nd ed., World Scientific, Hackensack, Singapore, 2006

[13] Siciliano, E., *et al.*, Comparison of PVT and NaI(Tl) Scintillators for Vehicle Portal Monitor Applications, Nuclear Instruments and Methods in Physics Research Section A: Accelerators, Spectrometers, *Detectors and Associated Equipment, 550* (2005), 3, pp. 647-674

[14] Takoudis, G., *et al.*, Spatial and Spectral Gamma-Ray Response of Plastic Scintillators Used in Portal Radiation Detectors; Comparison of Measurements and simulations, Nuclear Instruments and Methods in Physics Research Section A: Accelerators, Spectrometers, *Detectors and Associated Equipment, 599* (2009), 1, pp. 74-81

[15] Janda, J., *et al.*, The Comparison of Detection Parameters of Selected Photomultipliers Depending on the Shape of the Scintillator, *Nucl Technol Radiat, 33* (2018), 1, pp. 61-67

ANNEX

The easiest way to solve eq. (23) numerically is by using the Monte Carlo integration method. It is a particular Monte Carlo method that numerically computes a definite integral by using random numbers.

Let us assume an example case with n energy windows. To calculate the MDA value for some particular radionuclide, one needs to measure the response to the ambient radiation background (in terms of gross background counts per acquisition interval for each energy window) denoted as $\mu_1,\ldots,\mu_n$ and efficiencies for a given radionuclide (in terms of net counts per acquisition interval per activity) for each energy window denoted as $\varepsilon_1,\ldots,\varepsilon_n$.

The MDA value is then estimated iteratively by generating n sets of random values with the normal distribution – this represents the probability density function in the eq. (23). The ratio of n-tuples, for which $D^* \quad k_{1\ \alpha}^* (n)$ (representing the set   ), to the total number of generated n-tuples gives the non-detection probability. The goal of this algorithm is to find such n sets of random values, for which is the non-detection probability is equal to the required value β.

To achieve this, a parameter corresponding to the minimal activity increase step (denoted as δ) has to be set. For example, if the efficiency is given in net counts per acquisition interval per kBq and the δ were to be equal to 1, then the minimal resolution of the MDA would be 1 kBq. The MDA calculation is then described by the following pseudocode.

MDA calculation:

n number of energy windows

$\mu_1,\ldots,\mu_n$ gross background counts per acquisition interval for each energy window

$\varepsilon_1,\ldots,\varepsilon_n$ efficiency for a given radionuclide in terms of net counts per acquisition interval per activity for each energy window

δ minimal activity step

α false alarm probability

β non-detection probability

$k_{1\ \alpha}^* (n)$ quantile

i 0

repeat

    $i \quad i+\delta$

    $X_j \quad N(\mu_j + i\ \varepsilon_j, \mu_j + i\ \varepsilon_j)$ for $j = 1,\ldots, n$ (sets of generated random numbers)

    D^* value calculated by eq. (9) for each generated n-tuple

    R number of $(D^* \quad k_{1\ a}^* (n))$ divided by the number of generated n-tuples

until $R \quad \beta$

MDA i

return MDA

T. Grisa, *et al*.: On a Multidimensional Data Proessing Method for Radiation ...
Nuclear Technology & Radiation Protection: Year 2020, Vol. 35, No. 3, pp. 235-243

243

Томас ГРИСА, Даниел САС, Лубомир ГРИЦ

О ВИШЕДИМЕНЗИЈАЛНОЈ МЕТОДИ ОБРАДЕ ПОДАТАКА ЗА ПОРТАЛ МОНИТОРЕ ЗРАЧЕЊА

Са становишта националне безбедности, важно је открити транспорт радиоактивних материјала или потенцијалну радиоактивну контаминацију. Најчешће коришћени уређаји су портал монитори зрачења са пластичним сцинтилационим детекторима. Сигнал са таквих детектора обрађује се анализатором амплитуде који може раздвојити импулсе у неколико међусобно независних енергетских прозора, који представљају енергетске интервале гама зрачења. Због тога је најприкладнија метода процене употреба алгоритама за вишедимензијалну обраду. У овом раду описан је нови уопштени приступ осмишљен према својствима портал монитора зрачења. Садржи опис формула и цео алгоритам, као и поступак за одређивање одговарајућих критичних ограничења и граница детекције. Предвиђена расподела вероватноће за предложену методу прорачуна верификована је симулацијама и експерименталним мерењима. Алгоритам је такође упоређен са уобичајеним алгоритмом укупног бројања.

Кључне речи: йортал монитор зрачења, вишедимензијална обрада йодатака,
критично ограничење, граница детекције, сцинтилациони детектор,
анализатор амйлитуде